Electronic Supplementary Material (ESI) for RSC Applied Polymers.

Supporting information

Poly(L-glutamic acid) augments the transfection performance of lipophilic polycations by overcoming tradeoffs among cytotoxicity, pDNA delivery efficiency, and serum stability

Ram Prasad Sekar,[†] Jessica L. Lawson,[‡] Aryelle R.E. Wright,[¶] Caleb McGrath,[¶] Cesar Schadeck,[‡] Praveen Kumar,[§] Jian Tay,[‖] Joseph Dragovan,[‖] and Ramya Kumar[*,†,‡,¶]

[†]*Chemical and Biological Engineering, Colorado School of Mines, Golden, CO 80401*

[‡]*Materials Science, Colorado School of Mines, Golden, CO 80401*

[¶]*Quantitative Biosciences and Engineering, Colorado School of Mines, Golden, CO 80401*

[§]*Shared Instrumentation Facility, Colorado School of Mines, Golden, CO 80401*

[‖]*BioFrontiers Institute, University of Colorado, Boulder, CO*

E-mail: ramyakumar@mines.edu

Contents

1 1 H NMR and SEC characterization data for DIP50H50

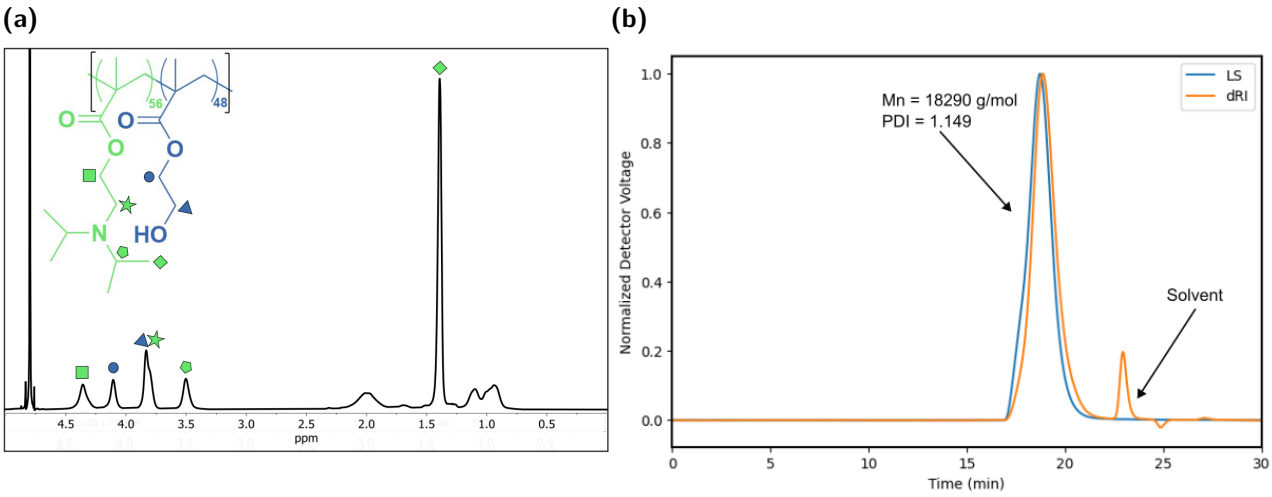

Figure S1. (a) 1 H NMR spectrum of p(DIPAEMA$_{56}$-*st*-HEMA$_{48}$) (DIP50H50) (b) Molecular weight distribution was determined using size exclusion chromatography with multi-angle light scattering.

2 Electrokinetic characterization and DLS data for uncoated and PGA-coated polyplexes in water

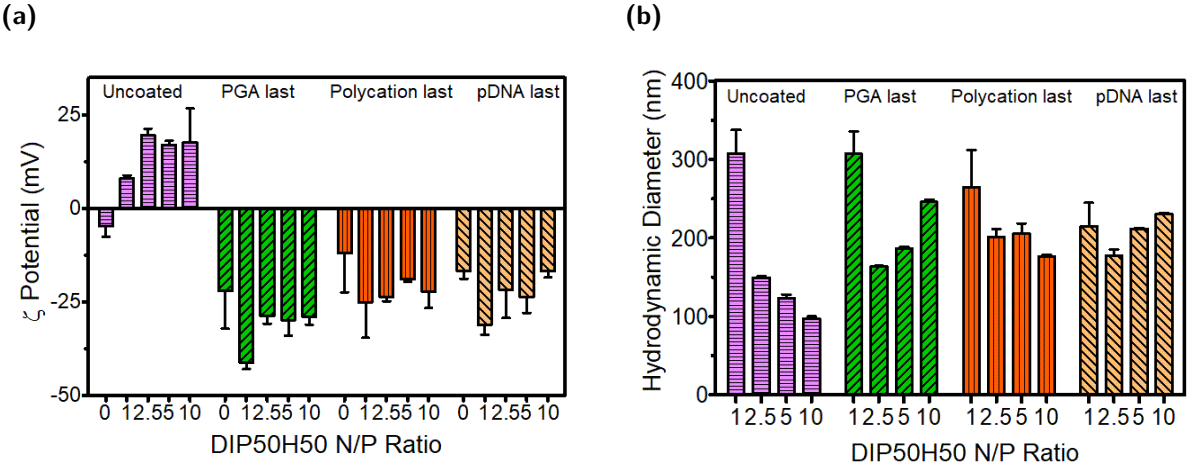

Figure S2. (a) ζ-potential values of uncoated polyplexes and PGA-coated polyplexes were compared. Uncoated polyplexes were cationic whereas PGA neutralized cationic charge across all N/P values and addition sequences (b) Dynamic light scattering showed that polyplex size decreased from 300 to 80 nm with increasing N/P ratio for uncoated polyplexes.

3 Supplemental circular dichroism spectra

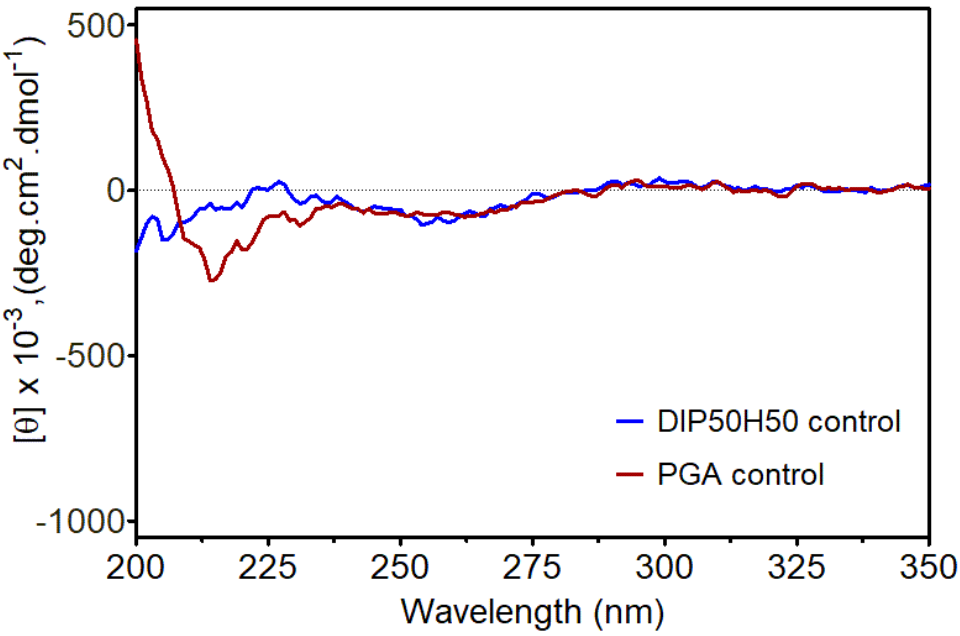

Figure S3. To verify that DIP50H50 and PGA do not generate any CD signals overlapping with pDNA, we collected control CD spectra. The PGA control exhibited an isodichoric point in the 200-220 nm region. As expected DIP50H50 did not produce any CD signal.

4 Transfection results for polycation last and pDNA last addition schemes

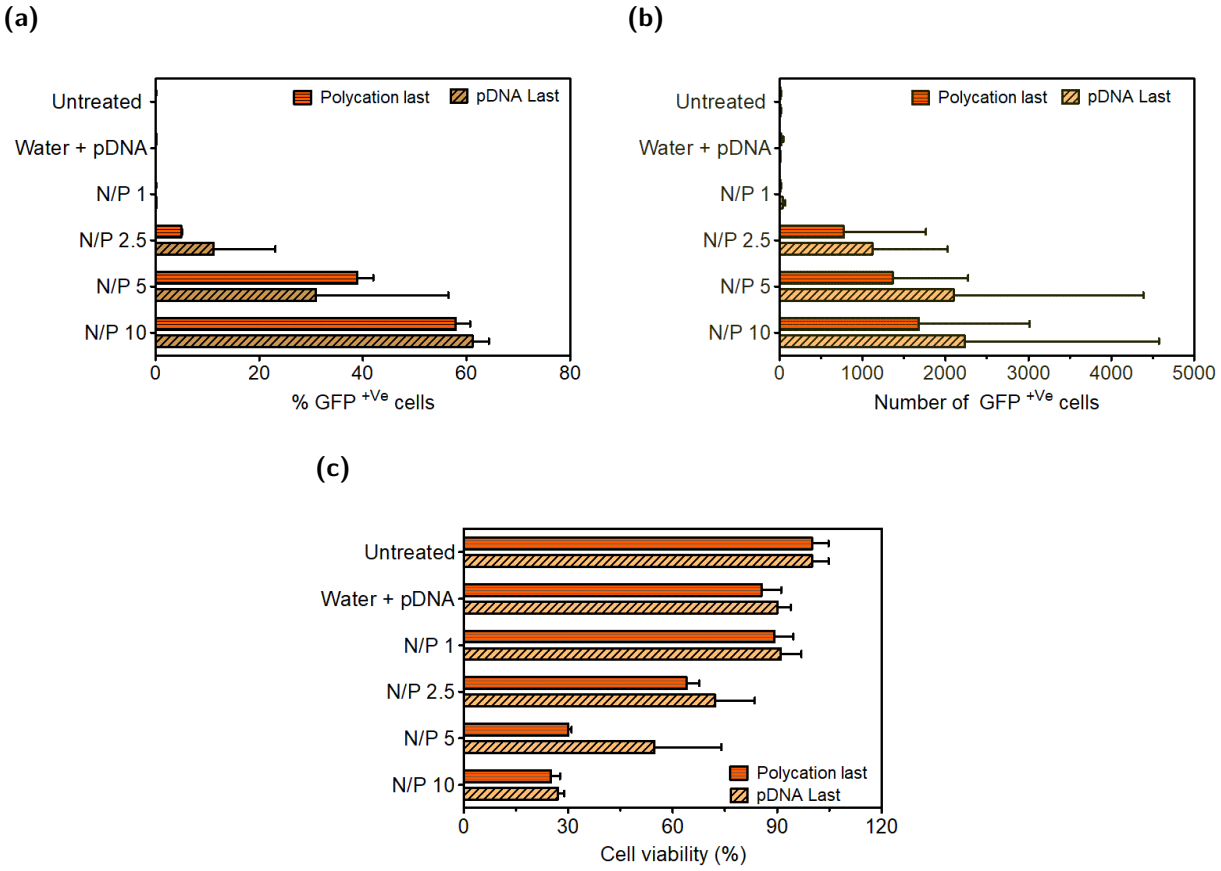

Figure S4. (a) Polycation last and pDNA last addition seque ces mediated efficient pDNA delivery (b) pDNA last led to a higher population of GFP^+ cells compared to polycation last (c) Both polycation last and pDNA last addition sequences exhibited cell viability comparable to PGA last polyplexes.

5 Supplemental transfection data for PGA last polyplexes

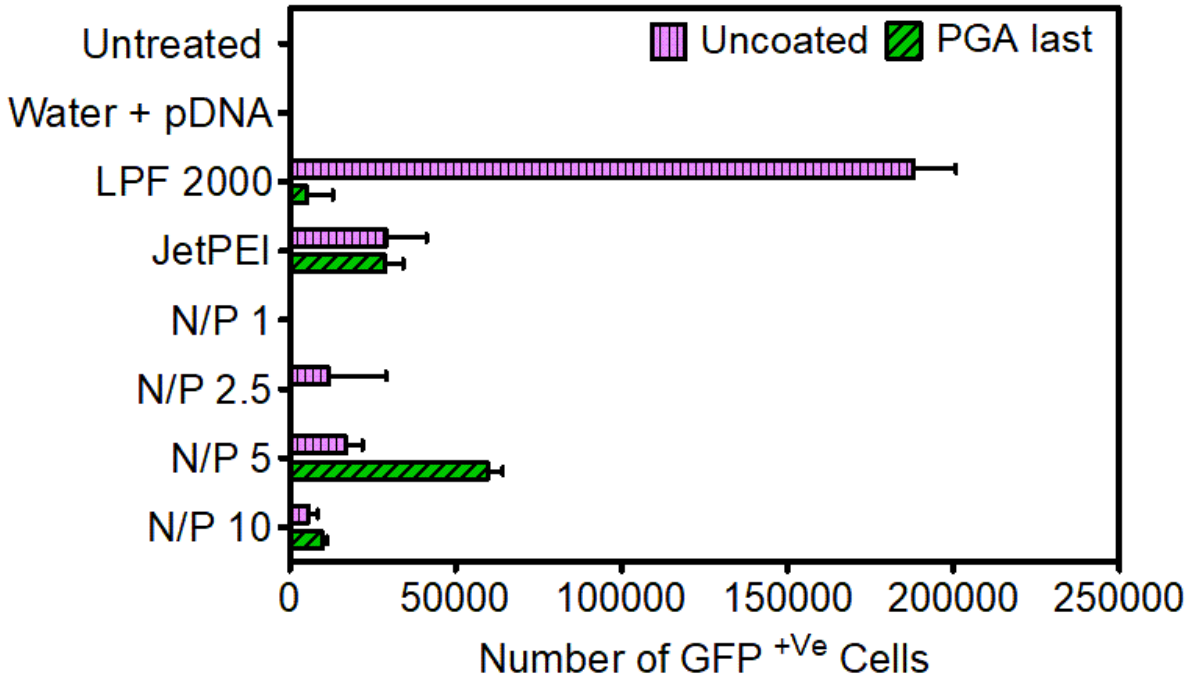

Figure S5. PGA-coated polyplexes generated a greater proportion of GFP+ cells than uncoated polyplexes.

6 Correlation analysis between transfection efficiency and cell viability

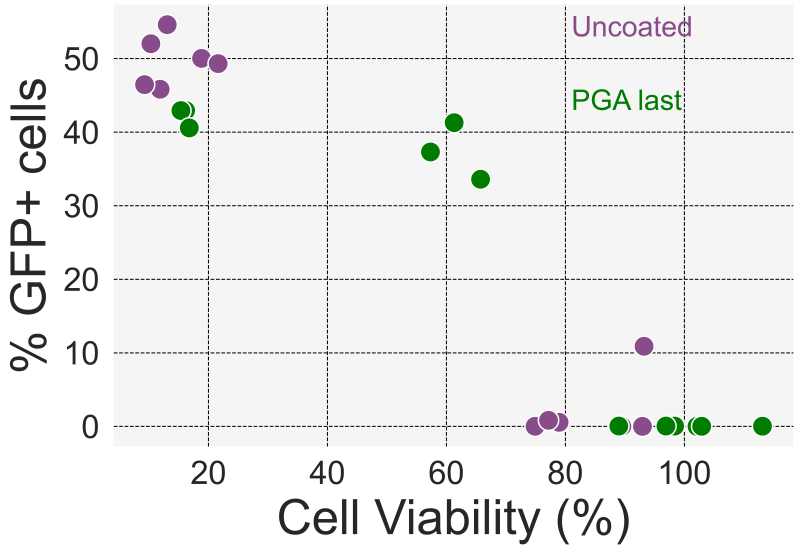

Figure S6. For uncoated polyplexes, transfection outcomes belonged to either the "low efficiency high viability" regime in the bottom right or the "high efficiency low viability" regime in the top left. PGA-coated polyplexes (N/P 5, center of the plot) mediated efficient transgene delivery while avoiding the severe cytotoxicity triggered by uncoated DIP50H50 polyplexes.

Table S1. Pearson's correlation coefficients (PCC) approached -1 for both uncoated and PGA-coated polyplexes, suggesting that high transfection efficiency is accompanied by severe toxicity. However, PCC values were slightly lower for PGA-coated polyplexes, indicating that PGA weakened the correlation between transfection efficiency and cytotoxicity.

Treatment	PCC	p-value	95% CI lower	95% CI upper
Uncoated	-0.96	4E-07	-0.99	-0.88
PGA last	-0.91	4E-05	-0.98	-0.71

7 Comparing the effect of PGA coating on the electrokinetic properties of JetPEI and DIP50H50 polyplexes

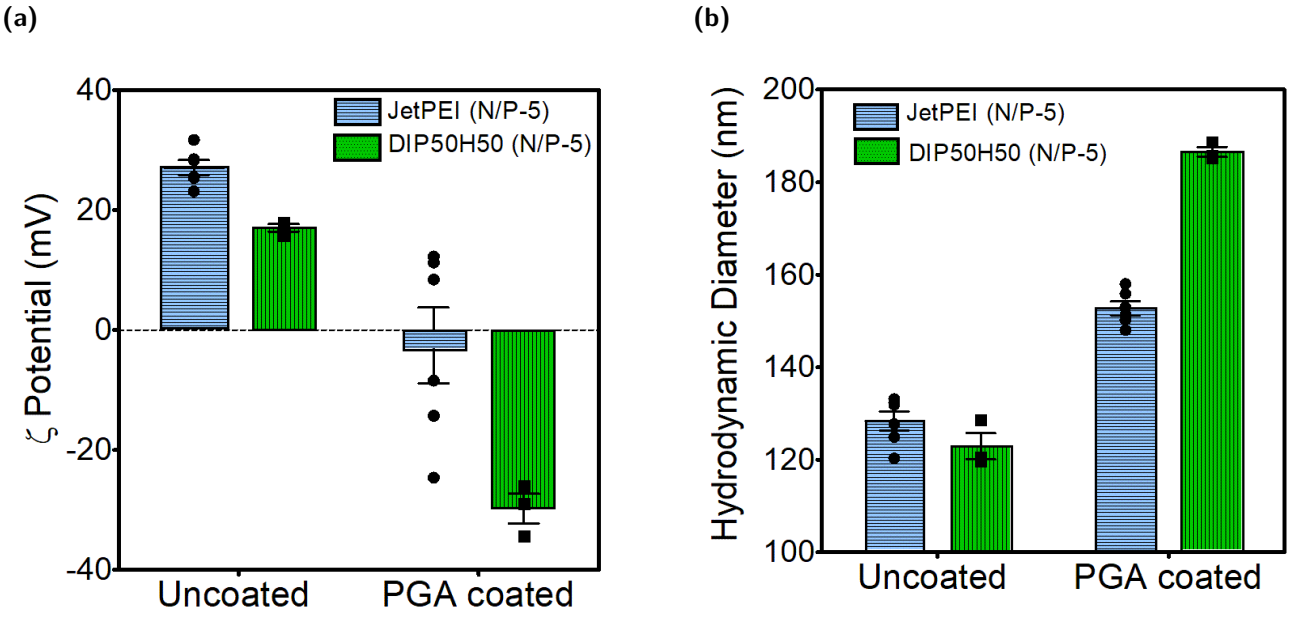

Figure S7. (a) Negative ζ-potential values for DIP50H50 polyplexes suggest that PGA was uniformly deposited. For JetPEI, ζ-potential values were in the neutral regime, suggesting that PGA did not coat polyplexes conformally (b) PGA-coated DIP50H50 polyplexes were larger than PGA-coated JetPEI polyplexes.

8 Polyplex interactions with 10% and 50% serum: Effect of addition sequence

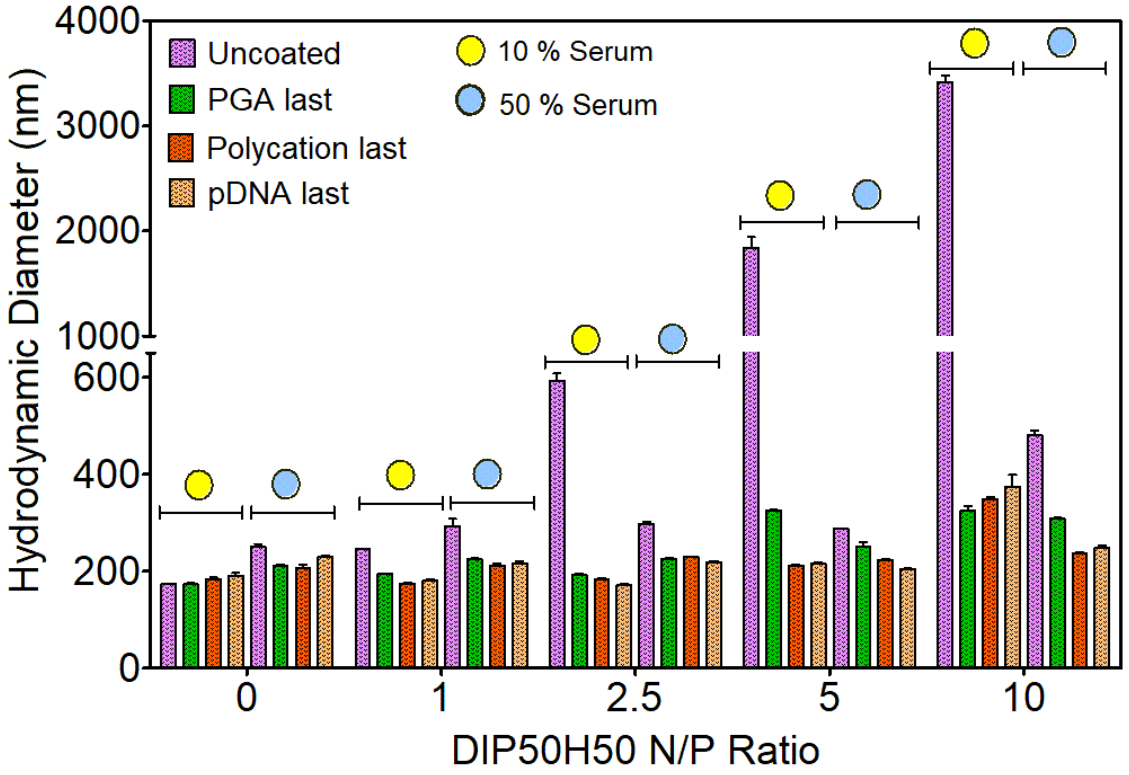

Figure S8. Dynamic light scattering measurements of uncoated and PGA-coated polyplexes in 10% or 50% human serum. Uncoated polyplexes aggregated severely, with the hydrodynamic diameter approaching 3 μm. In contrast, PGA-coated polyplexes resisted aggregation in serum, irrespective of addition sequence.

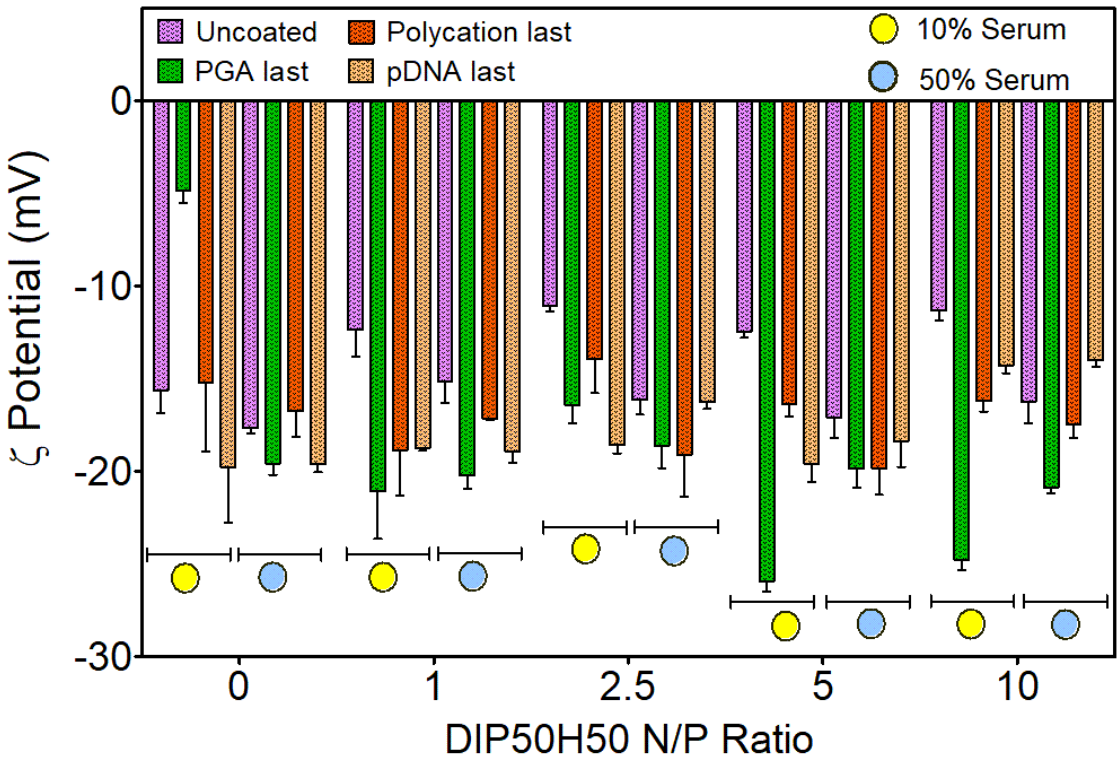

Figure S9. Uncoated and PGA-coated polyplexes were negatively charged across all N/P ratios in 10% or 50% serum.

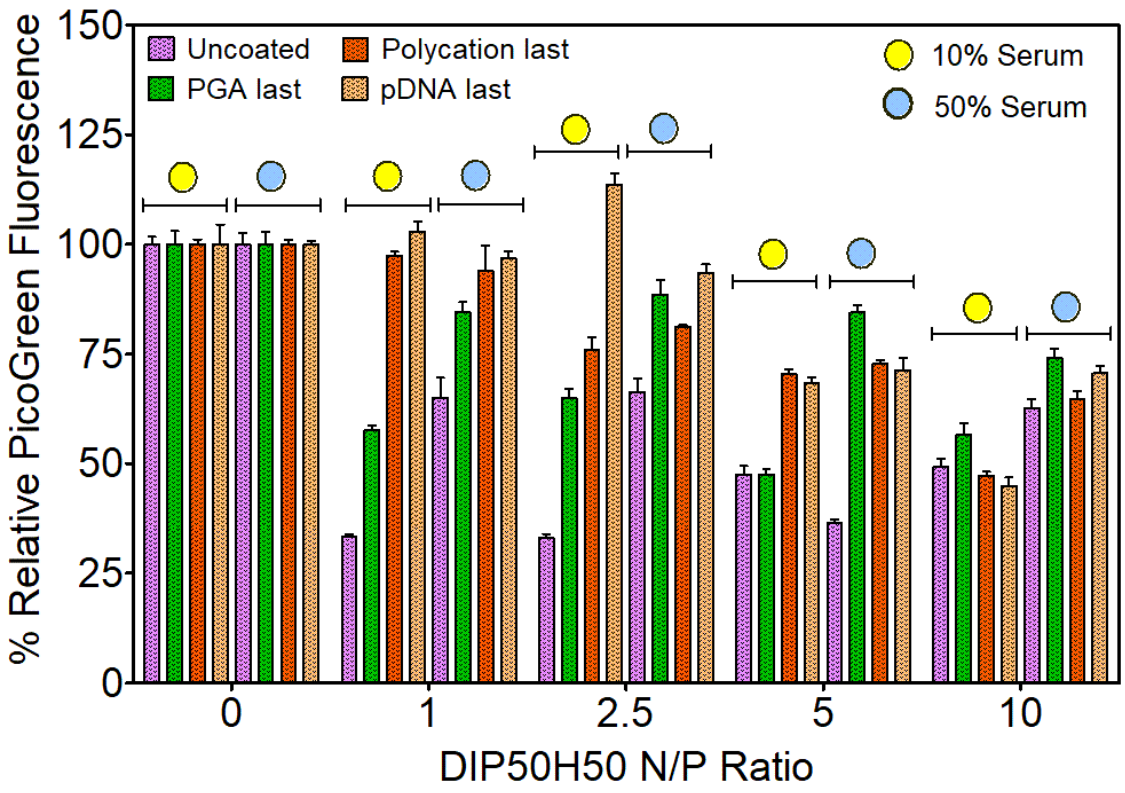

Figure S10. PGA last polyplexes retained pDNA in the presence of serum (10% or 50% v/v), whereas serum proteins triggered pDNA release for polycation last or pDNA last polyplexes.

9 Supplemental transfection data for PGA last polyplexes as a function of serum content

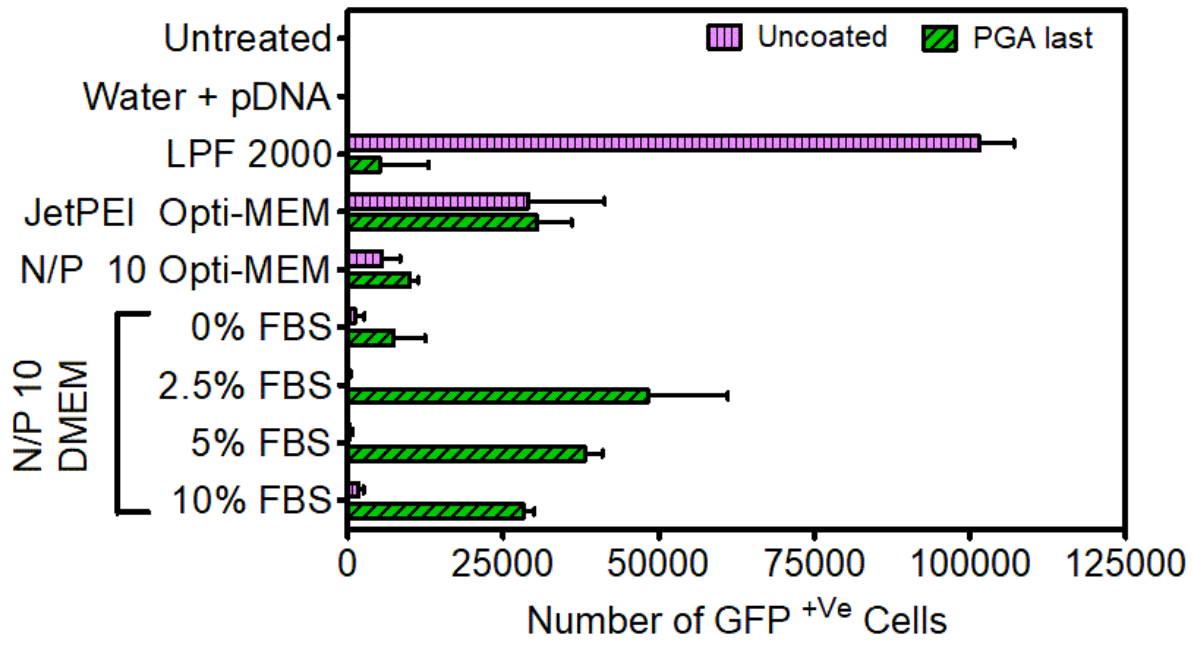

Figure S11. PGA last polyplexes tolerated serum better than uncoated polyplexes, expanding the population of GFP^+ cells.

10 Supplemental confocal images

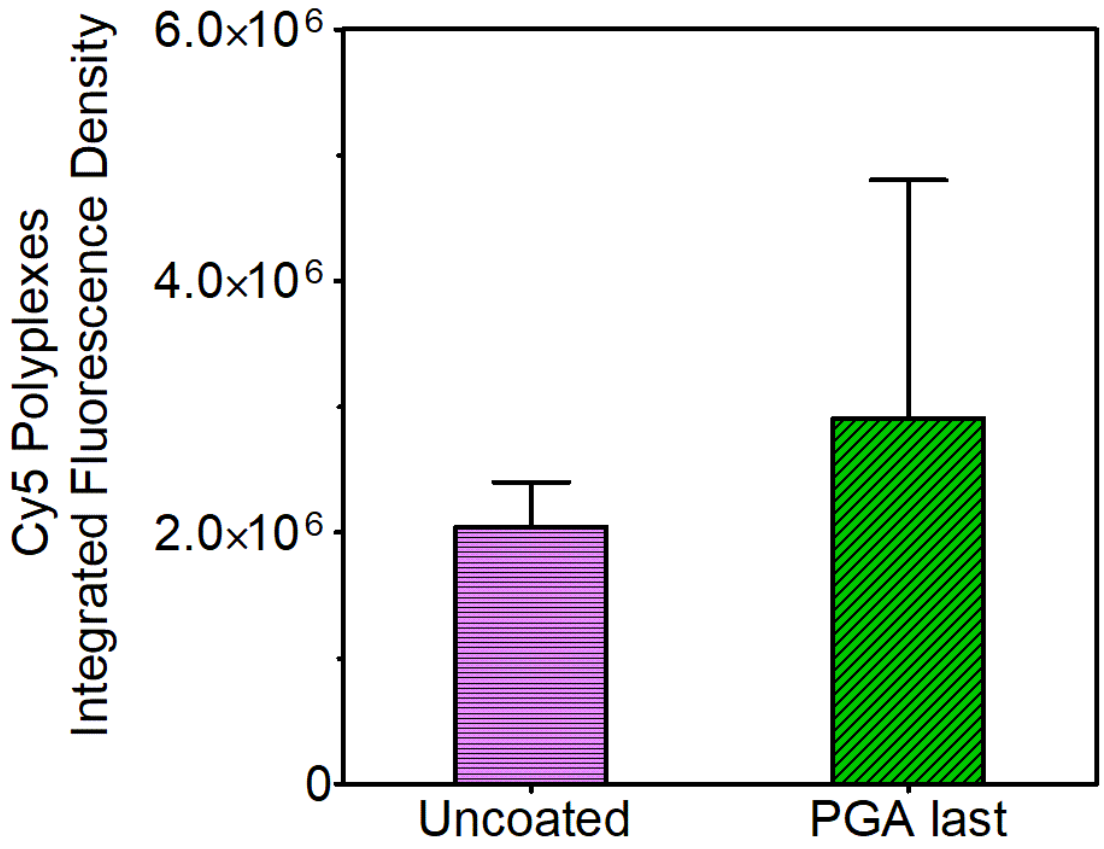

Figure S12. The integrated fluorescence intensity of Cy5 polyplexes was higher in the PGA-coated treatment than the uncoated group.

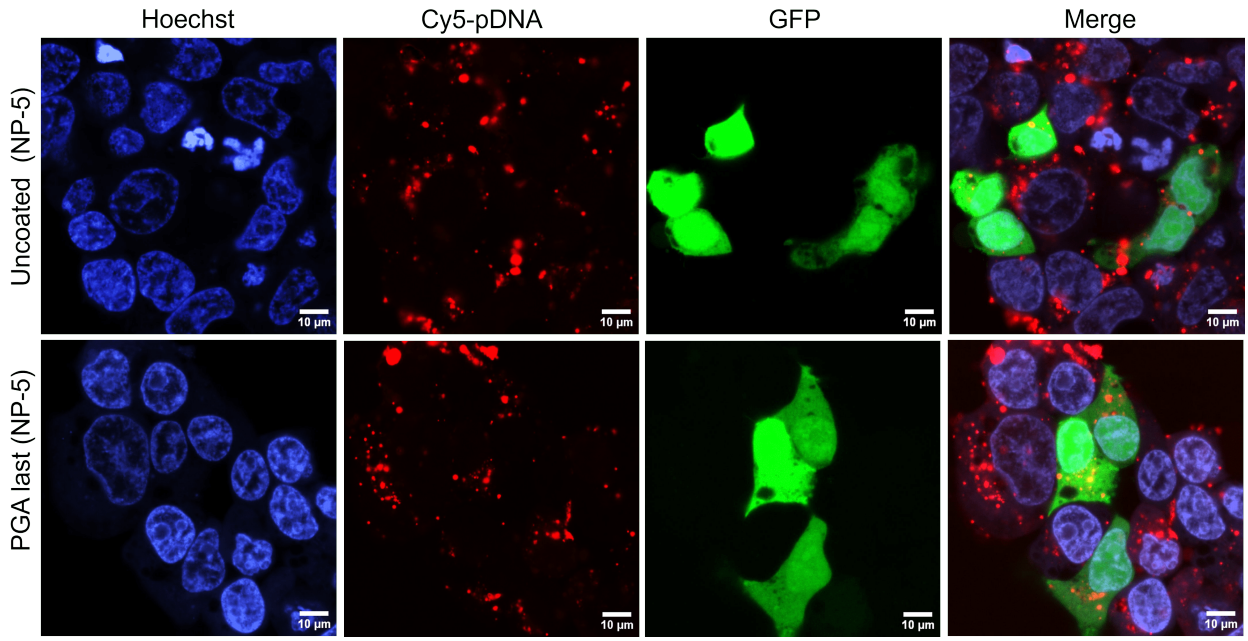

Figure S13. Two-dimensional confocal projections of uncoated and PGA last polyplexes. Nuclei are stained with Hoechst (blue), polyplexes labeled with Cy5 (red fluorescence), transfected cells express GFP (green). The scale bar is 10μm.

11 Supplemental hemolysis data

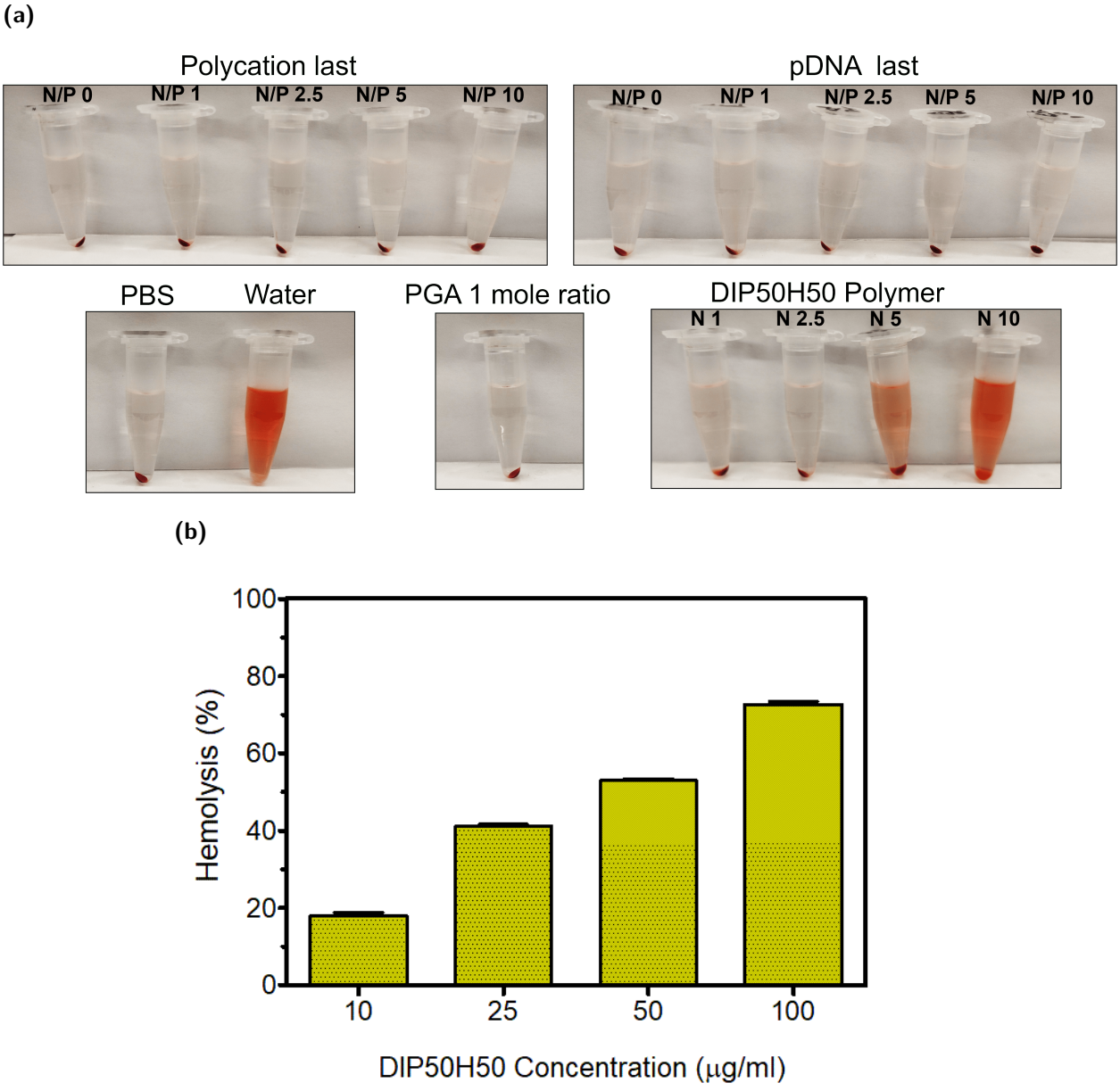

Figure S14. (a) Visual assessment of hemolysis triggered by PGA-coated polyplexes, PGA, and DIP50H50. Water and PBS served as negative and positive controls respectively (b) DIP50H50 (polymer without pDNA) triggered concentration-dependent RBC lysis.

12 Flow cytometry gating schemes

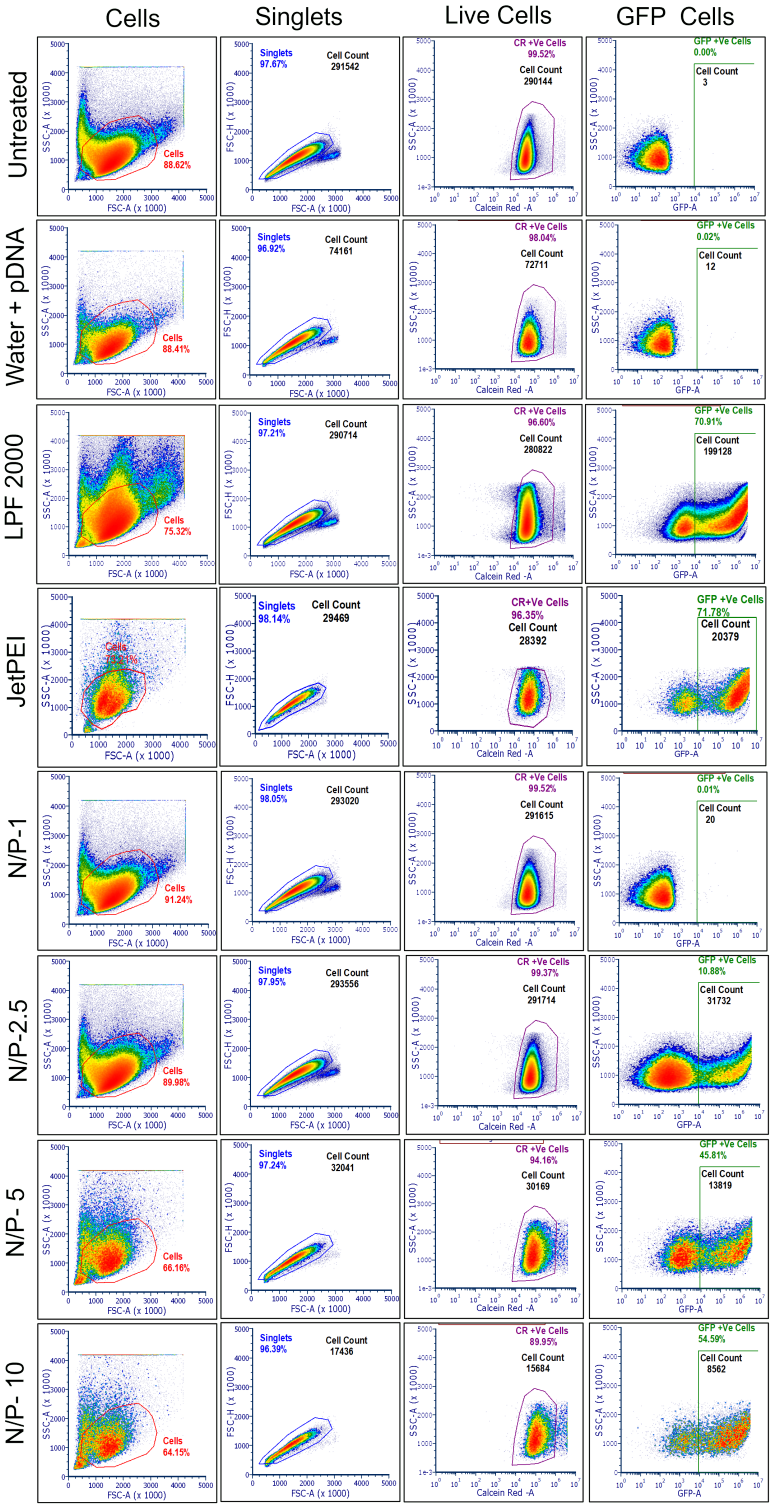

Figure S15. Flow cytometry gating schemes for uncoated samples analyzed in Figure 2 in the main manuscript

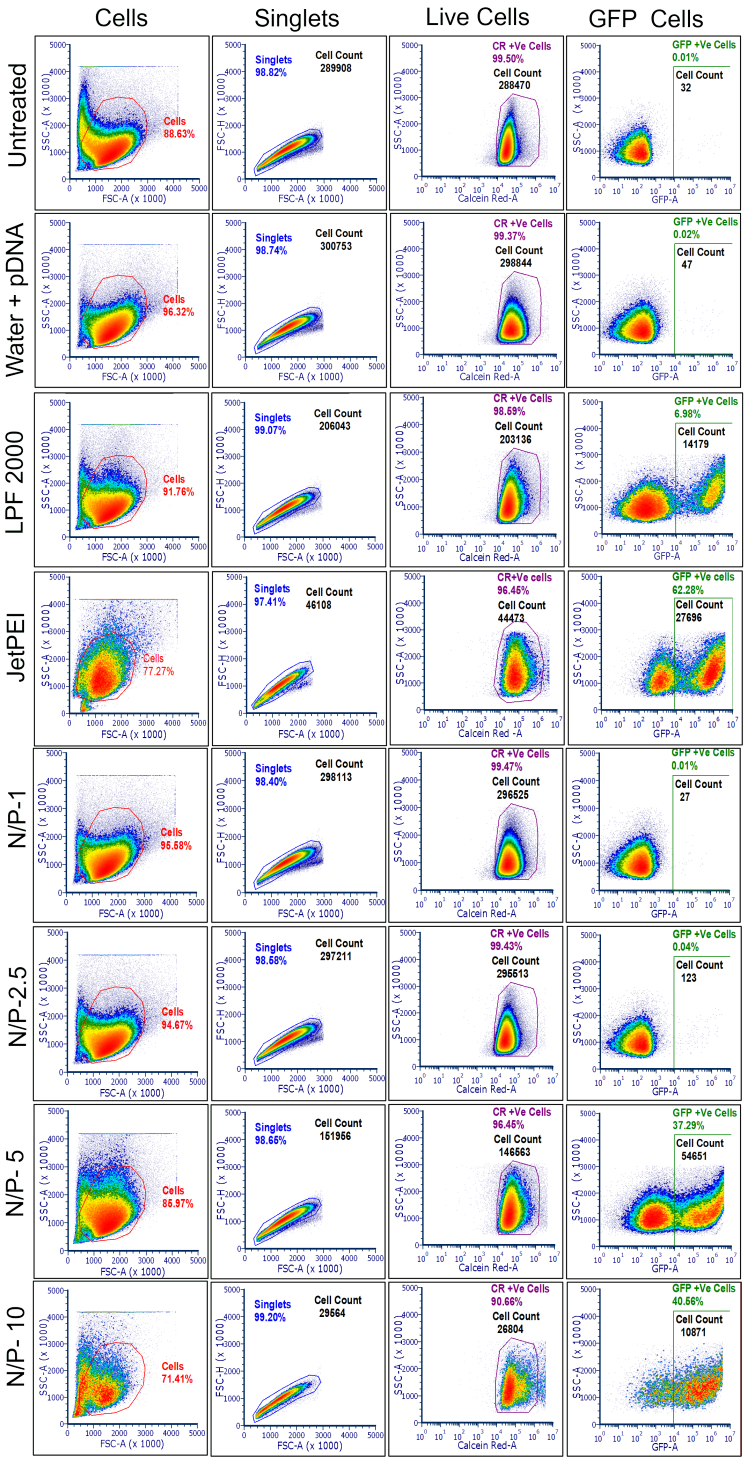

Figure S16. Flow cytometry gating schemes for PGA-coated samples analyzed in Figure 2 in the main manuscript

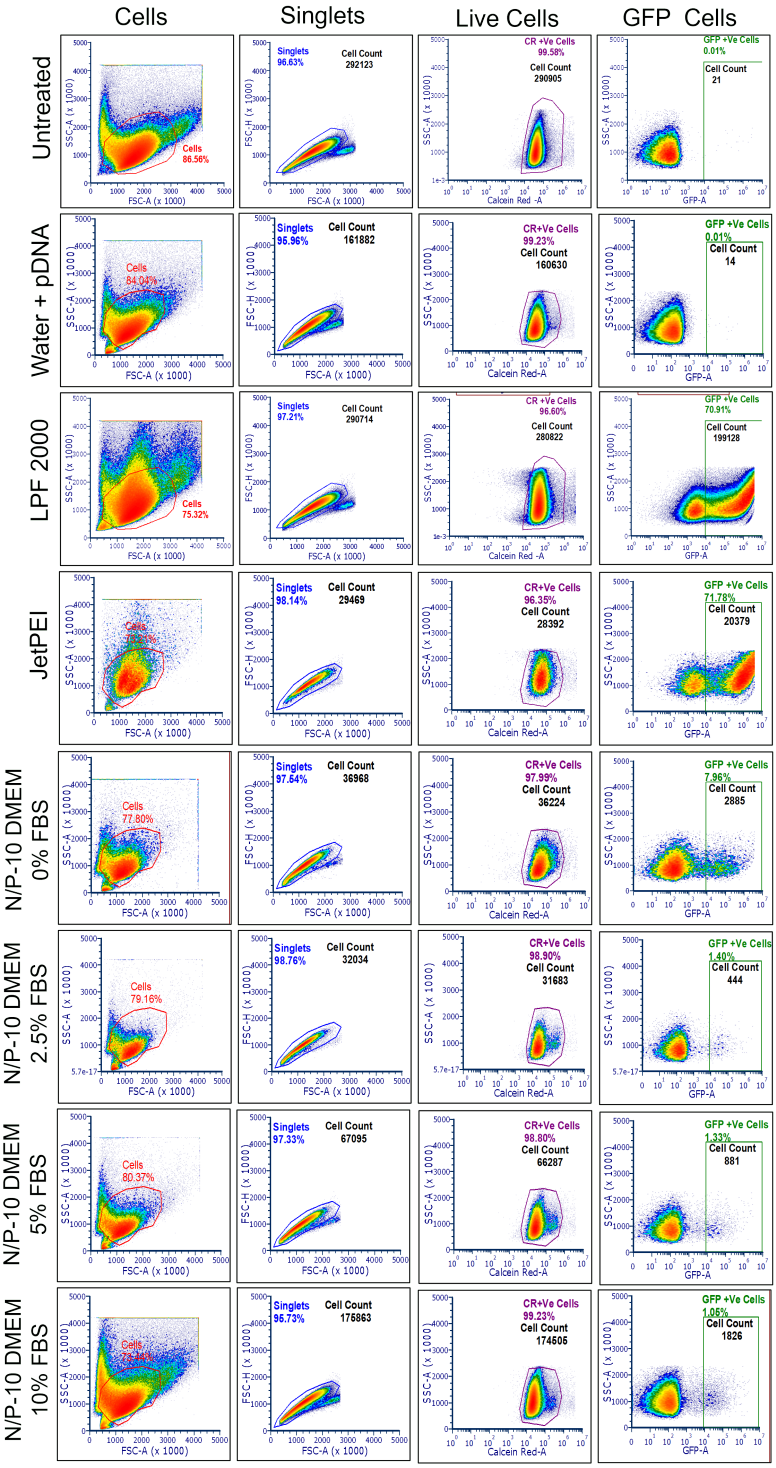

Figure S17. Flow cytometry gating schemes for uncoated samples analyzed in Figure 4B in the main manuscript

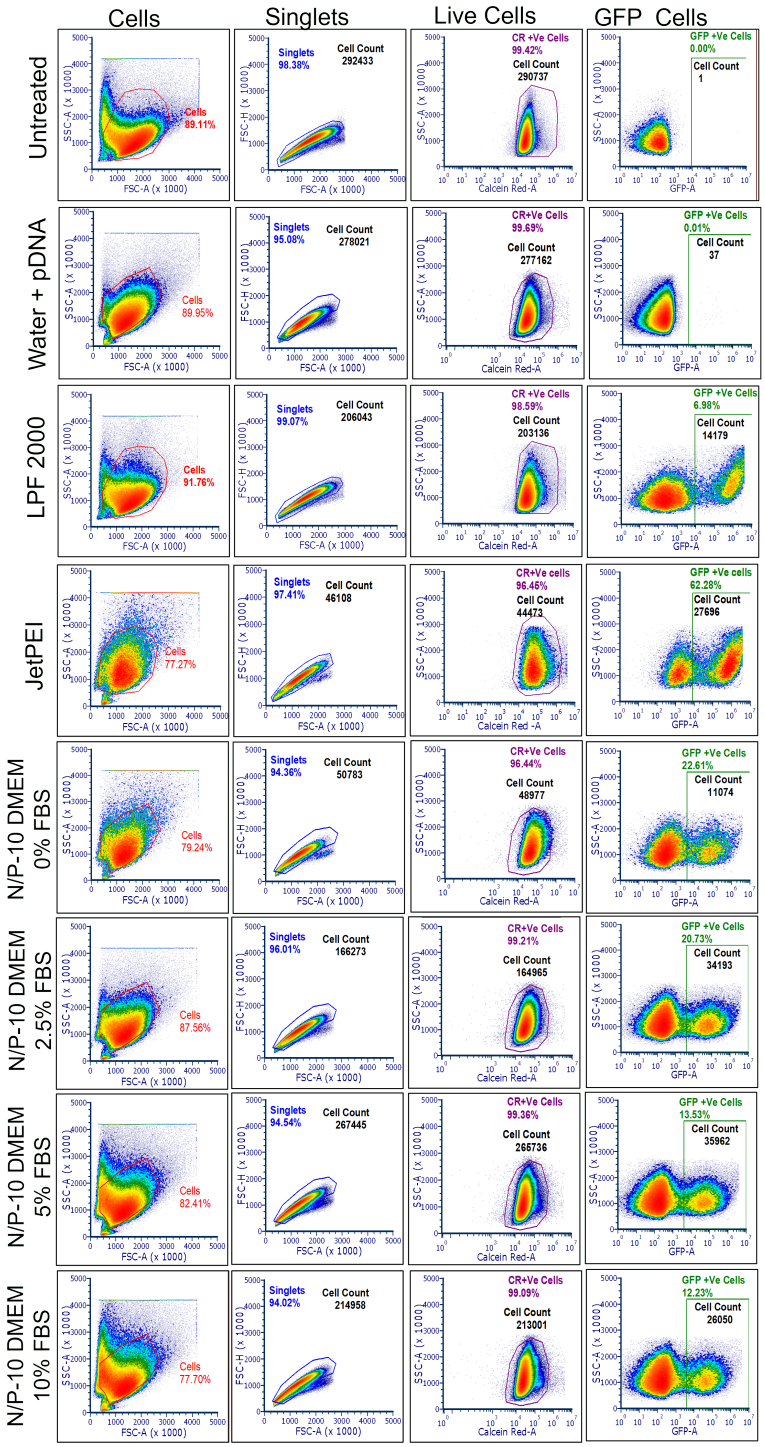

Figure S18. Flow cytometry gating schemes for PGA-coated samples analyzed in Figure 4B in the main manuscript

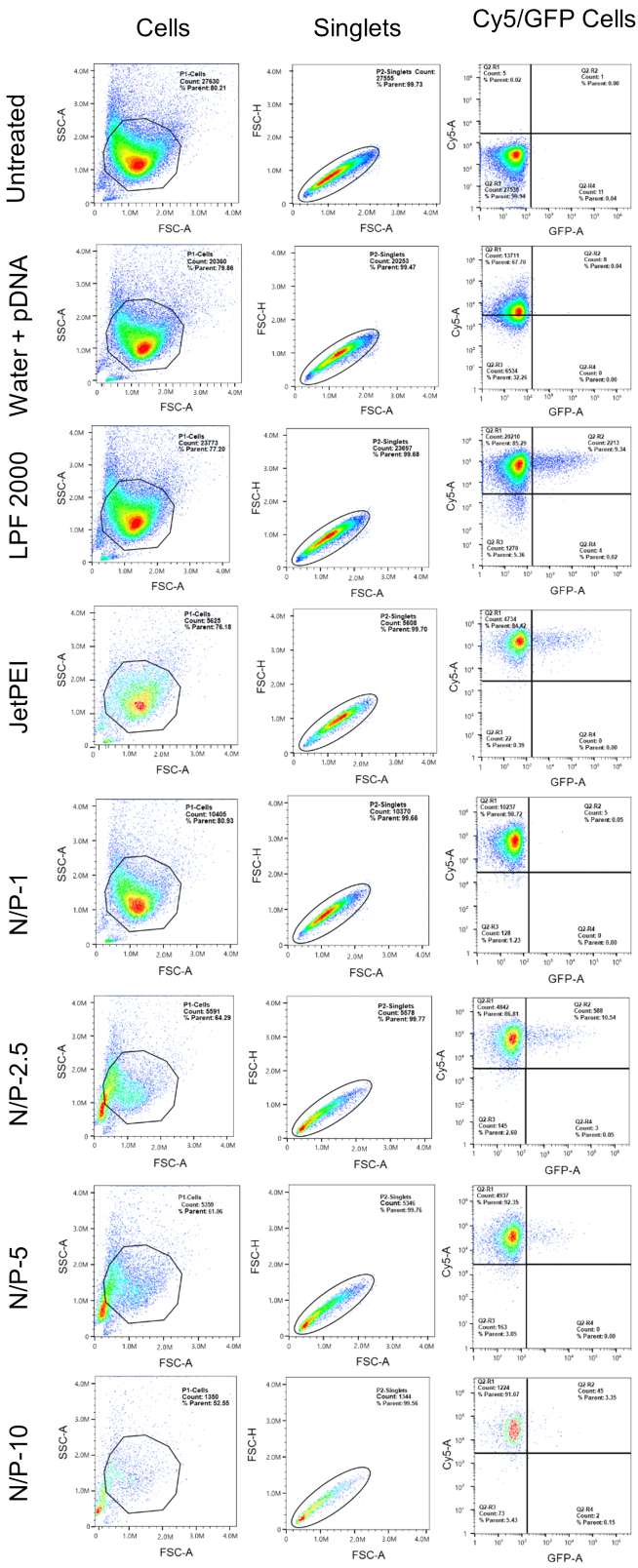

Figure S19. Flow cytometry gating schemes for uncoated samples analyzed in Figure 4D in the main manuscript

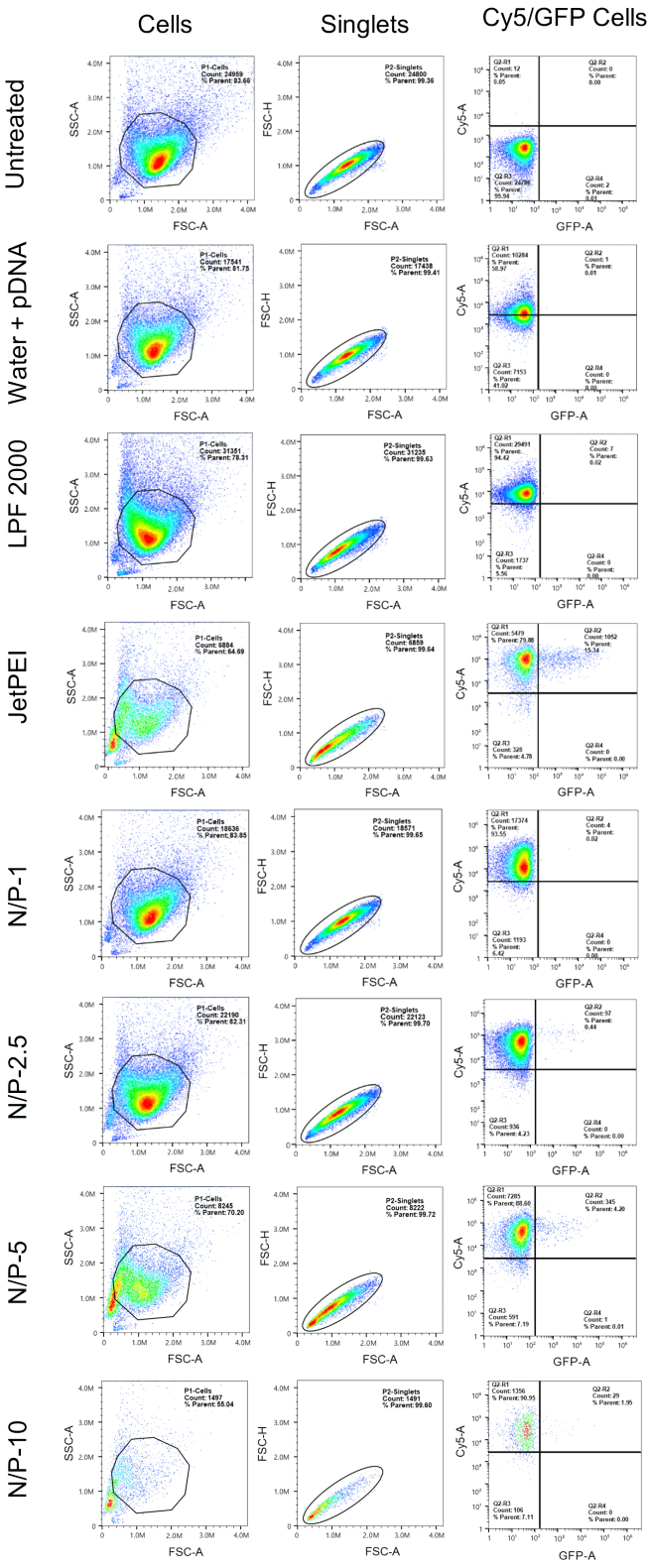

Figure S20. Flow cytometry gating schemes for PGA-coated samples analyzed in Figure 4D in the main manuscript

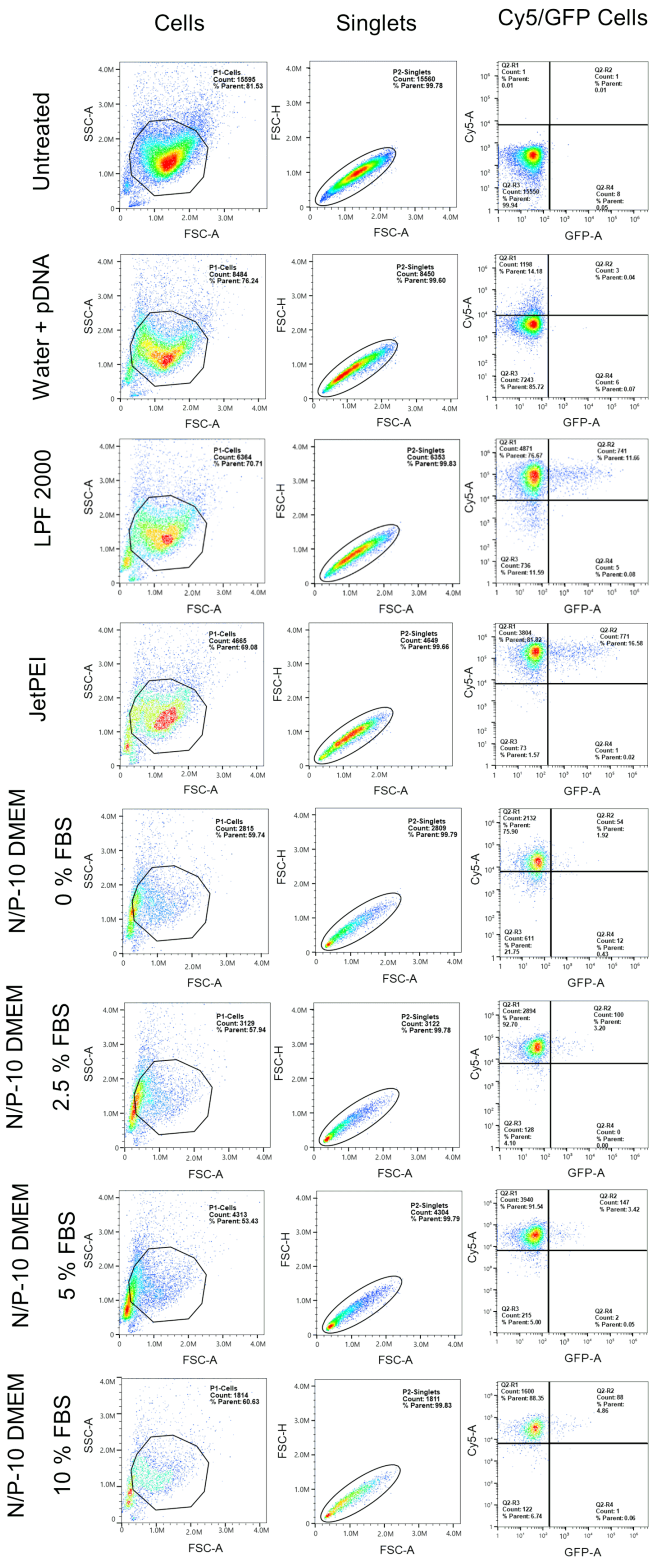

Figure S21. Flow cytometry gating schemes for uncoated samples analyzed in Figure 4E in the main manuscript

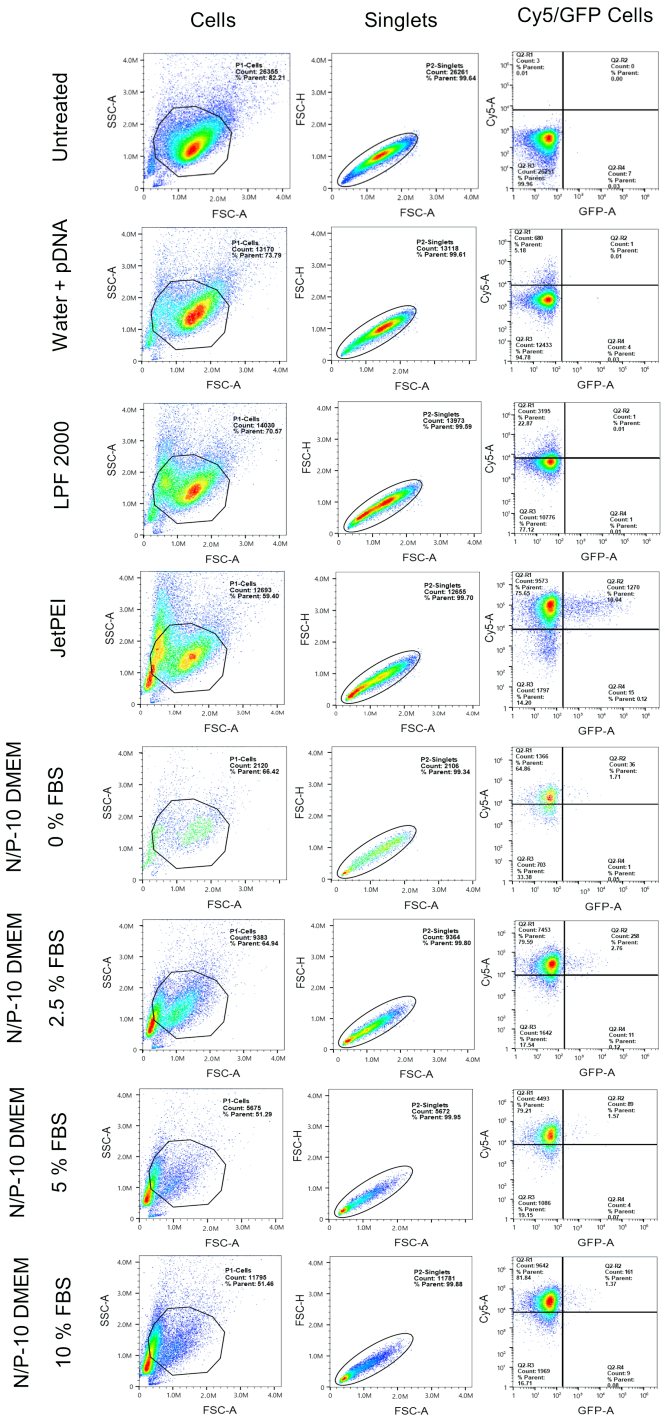

Figure S22. Flow cytometry gating schemes for PGA-coated samples analyzed in Figure 4E in the main manuscript